IOP Conf. Series: Materials Science and Engineering **739** (2020) 012038 doi:10.1088/1757-899X/739/1/012038

Numerical Analysis on Seismic Performance of a New Type of Fully Assembled Beam-Column Joints

W Zhai[1], W Jiang[1], J H Yang[1], J F Yang[2, 3], K Qu[2], L Chen[2]

[1]PowerChina Hubei Electric Engineering Corporation Limited, Wuhan, 430040
[2]School of Civil Engineering, Xi'an University of Architecture & Technology, Xi'an, 710055, China
[3]Key Lab of Structural Engineering and Earthquake Resistance, Ministry of Education (XAUAT), Xi'an, 710055, China

yjf9807@126.com

Abstract. To investigate the seismic performance of a new type of fully assembled beam-column joints, finite element models are established by ABAQUS with the nonlinear and geometric nonlinear effects considered to simulate 5 joints based on the quasi-static test. Through the comparison between finite element analysis and experimental results, the validity of finite element models is verified. Then the correlation parameters and their effects on the seismic performance of joints are analysed.

1. Introduction

Assembled steel structure building systems have rapidly developed under the promotion of national policies and developed more improved, modular and industrialized residential building systems based on the traditional steel structures [1]. Assembled steel structures refer to the multi-high-rise buildings constructed with the industry-produced steel columns and beams as framework and the lightweight, heat insulating and high-strength wall materials as enclosure system [2], in which the beam-column joints are very important to the overall mechanical behaviour of assembled steel structures [3]. At present, a lot of researches have been done on the assembled beam-column joints at home and abroad [4-9]. Literature [4] and [5] introduce a new type of beam-column joint connected with T-plate and high-strength bolt to improve the assembly efficiency of steel structures. In literature [6] and [7], the assembly of joint is further improved through the application of single side locking bolts. However, too many bolt holes on the columns of above-mentioned joints markedly reduce the bearing capacity. To solve this problem, a standard joint with well industrialization production and high seismic performance is proposed by the AISC and analysed in literature [8] and [9]. In this paper, finite element models of a new type of assembled beam-column joint based on the pseudo-static test are established, and the effects of correlation parameters on the seismic performance of joint are analysed and compared to provide a certain reference for the design joints.

2. Establishment of finite element model

2.1. Joint specimen design

As presented in figure 1, the new type of beam-column joint used for assembled steel structure is composed of rectangular tube column, H-beam, channel plate, angle iron, T-plate and high-strength bolt.

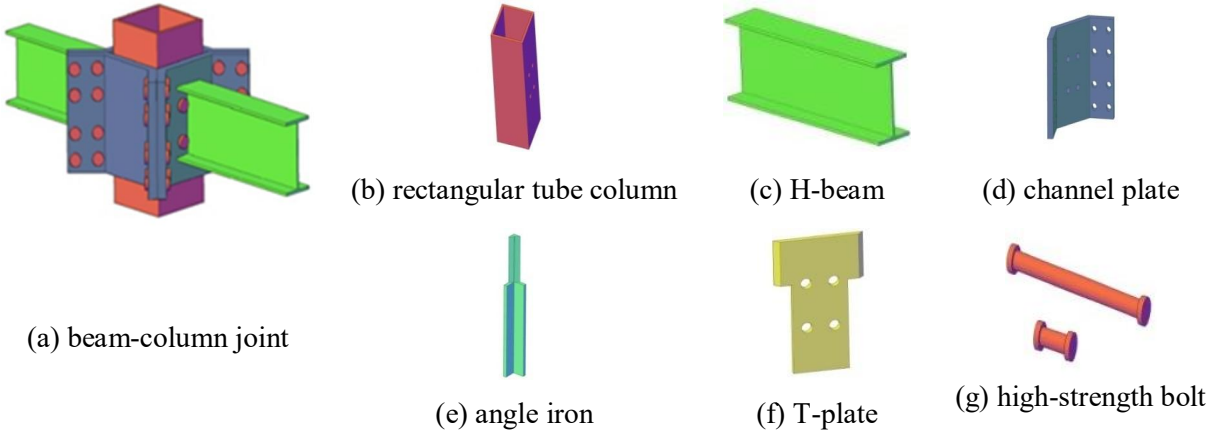

(a) beam-column joint (b) rectangular tube column (c) H-beam (d) channel plate (e) angle iron (f) T-plate (g) high-strength bolt

Figure 1. Beam-column joint and components.

Welded rectangular steel tube column and H-shaped steel beam are connected by 10.9-grade friction-type high-strength bolts, and all components are produced with Q345B steel. In literature [10], pseudo-static test with the same axial compression ratio of 0.2 was conducted on 5 scale models of 1:2 ratios. Specific dimensions of these specimens are shown in table 1.

Table 1. Specific dimensions of specimens.

Group	Dimension		Thickness		Bolt specification			RBS
	Column	Beam	T-plate	Angle iron	Channel plate	Shearing bolt	Bending bolt	
JD1	200×10	H200×100×5.5×8	12	12	28	M20×4	M24×8×2	NO
JD2	200×10	H200×100×5.5×8	12	12	28	M16×4	M24×8×2	NO
JD3	200×10	H200×100×5.5×8	12	12	20	M20×4	M24×8×2	NO
JD4	200×10	H200×100×5.5×8	12	12	28	M20×4	M20×8×2	NO
JD5	200×10	H200×100×5.5×8	12	12	28	M20×4	M24×8×2	YES

2.2. Finite element model

Finite element models corresponding to the 5 beam-column joints are established by ABAQUS and the finite element analysis results are compared with the testing results to prove the validity of the finite element model. The hysteretic and skeleton curves of 5 joints obtained from finite element models and tests are compared in figure 2 and 3, respectively.

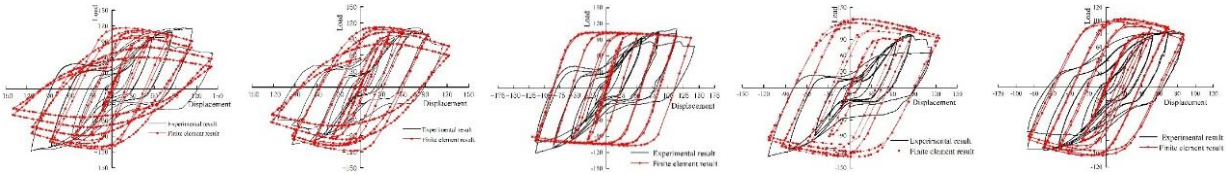

(a) JD1 (b) JD2 (c) JD3 (d) JD4 (e) JD5

Figure 2. Experimental and finite element hysteretic curves.

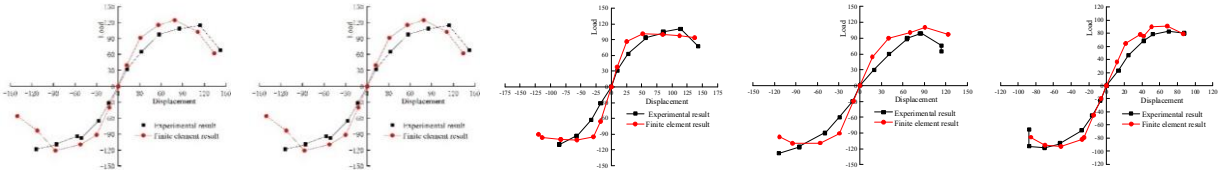

(a) JD1 (b) JD2 (c) JD3 (d) JD4 (e) JD5

Figure 3. Experimental and finite element skeleton curves.

The finite element results agree well with the experimental results because both skeleton curves are close to each other and present converted S shape, indicating that specimens has gone through 3 stages of elastic, elastoplastic and plastic failure under the action of low frequency cyclic loading. Besides, comparisons of the failure modes and the parameters between finite element analysis and experimental results are presented in figure 4 and table 2, respectively.

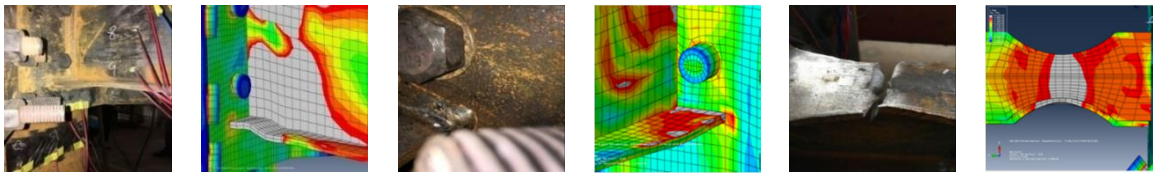

(a) Beam flange buckling (b) Beam flange tearing (c) Beam flange shrinking

Figure 4. Experimental and finite element failure modes.

Table 2. Comparison of the parameters between experimental results and finite element analysis.

Group	Yield					Ultimate				
	Experimental		Finite element		Ratio	Experimental		Finite element		Ratio
	P_{yE} /kN	Δ_{yE} /mm	P_{yF} /kN	Δ_{yF} /mm	P_{yF}/P_{yE}	P_{uE} /kN	Δ_{uE} /mm	P_{uF} /kN	Δ_{uF} /mm	P_{uF}/P_{uE}
JD1	98.4	58.8	106.4	46.0	1.08	118.6	114.0	123.9	79.2	1.04
JD2	89.2	48.4	94.1	39.6	1.05	110.2	76.0	103.3	57.8	0.94
JD3	90.5	57.3	89.0	30.0	0.98	121.1	114.0	101.2	83.6	0.84
JD4	87.9	56.9	92.8	47.4	1.06	128.6	114.0	111.4	90.6	0.87
JD5	69.5	37.5	79.0	37.9	1.14	95.2	70.0	90.7	68.9	0.95

In table 2, P_{yE} is the test yield load, Δ_{yE} is the test yield displacement, P_{yF} is the finite element yield load, Δ_{yF} is the finite element yield displacement, P_{uE} is the test ultimate load, Δ_{uE} is the test ultimate displacement, P_{uF} is the finite element ultimate load and Δ_{uF} is the finite element ultimate displacement. The difference less than 10% between finite element and experimental results can verify the accuracy of modelling, and thus the finite element simulation can be used to study the performance of joints.

3. Parameter analysis

3.1 Ratio of axial compression stress to strength

4 finite element models (Group JD-1) with different axial compression ratios (0.2, 0.4, 0.6 and 0.8) are designed to study the relation between the ratio of axial compression stress to strength and the seismic performance.

3.1.1. Stress analysis. In figure 5, JD-1 presents a typical failure mode that the channel plate is destroyed earlier than beam and column. That is, the joint fails before members. The ultimate failure

mode of joint is the destruction of channel plates and the local buckling of beam with a small axial compression ratio, as well as the failure of channel plates and column with large ratio.

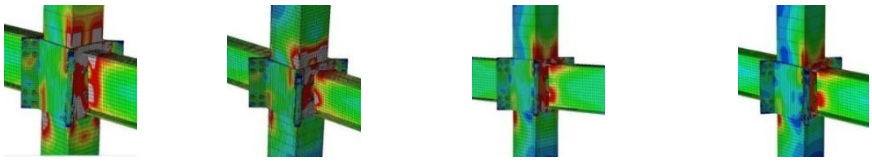

(a) JD-1-0.2 (a) JD-1-0.4 （c）JD-1-0.6 （d）JD-1-0.8

Figure 5. JD-1's Mises stress nephogram at the limited state of bearing capacity.

3.1.2. Skeleton and hysteretic curve. The skeleton and hysteretic curves of JD-1's column top loading point are drawn in figure 6 and 7, respectively. When the axial compression ratio increases from 0.2 to 0.8, the skeleton curves are in good agreement, while the hysteretic curves gradually shrink, which indicates the stepwise reduction of energy dissipation capacity.

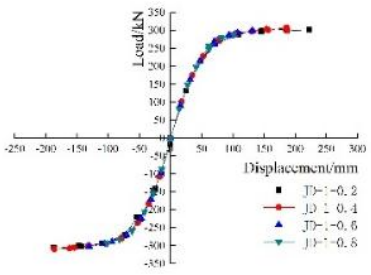

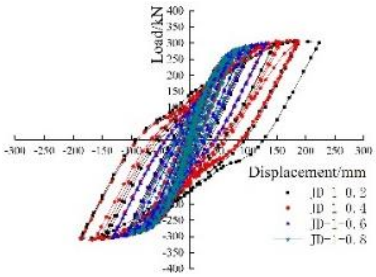

Figure 6. JD-1's skeleton curves. **Figure 7.** JD-1's hysteretic curves.

3.1.3. Ductility and energy dissipation capacity. As shown in table 3, when the ratio of axial compression stress to strength is less than 0.4, ductility coefficients are all greater than 3, indicating the good ductility of joints. Because the ductility coefficient decreases with the increase of axial compression ratio, high axial compression ratio can greatly weaken the ductility of joints. Besides, those energy dissipation coefficients below 2 correspond to passive energy dissipation modes that the channel plate bends before the beam yields fully.

Table 3. Ductility and energy dissipation capacity of JD-1.

No.	Axial compression ratio	Ductility coefficient μΔ	Energy dissipation coefficient Ce	Failure mode
JD-1-0.2	0.2	3.34	1.42	Channel plate and column core region buckling
JD-1-0.4	0.4	3.06	1.32	Channel plate and column core region buckling
JD-1-0.6	0.6	2.33	0.87	Channel plate buckling
JD-1-0.8	0.8	2.07	0.68	Channel plate buckling

3.2. Thickness of channel plate

3.2.1. Stress analysis. The Mises stress nephogram of JD-2 is shown in figure 8. As the thickness of channel plate increases, the stiffness grows accordingly, and increasingly radical plastic deformation appears in column and beam intensively. The failure mode of joint gradually changes from the buckling of channel plate to the formation of plastic hinge at the beam end, and the buckling of channel plate and column tends to aggravate.

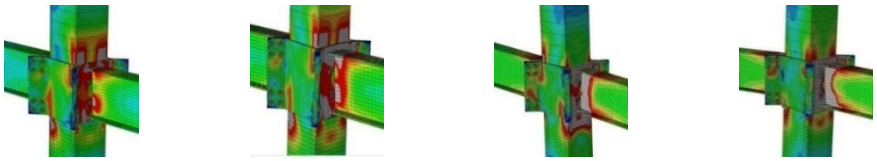

(a) JD-2-20 (b) JD-2-25 (c) JD-2-30 (d) JD-2-35

Figure 8. JD-2's Mises stress nephogram at the limited state of bearing capacity.

3.2.2. Skeleton and hysteretic curve. The skeleton and hysteretic curves of JD-2's column top loading point are drawn in figure 9 and 10, respectively. With the thickness of channel plate increasing, the hysteresis loop expands gradually, indicating the reinforcement of energy dissipation capacity. Meanwhile, the deformation capacity of joint is enhanced, but joint begins to shrink and slip with the increase of loading displacement. This is mainly because bolts tend to loosen under the action of low frequency cyclic loading when used for fully bolted joint and there is a smooth stage when the load remains while the displacement decreases in the unloading process after the channel plate being pulled open.

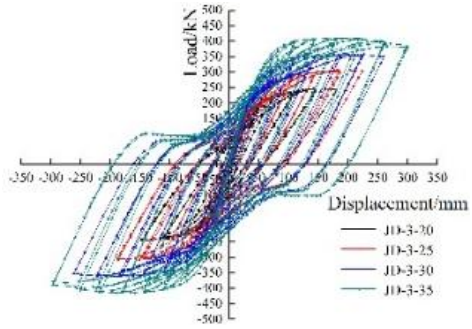

Figure 9. JD-2's hysteretic curves.

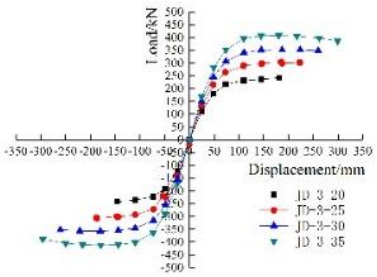

Figure 10. JD-2's skeleton curves.

3.2.3. Ductility and energy dissipation capacity. As shown in table 4, when the thickness of channel plate grows from 20mm to 35mm, the ductility coefficient has a sharp rise, indicating that the increase of channel plate thickness can strengthen the ductility of joint efficiently.

Table 4. Ductility and energy dissipation capacity of JD-2.

No.	Axial compression ratio	Ductility coefficient μΔ	Energy dissipation coefficient Ce	Failure mode
JD-2-20	0.2	3.01	1.00	Channel plate and column core region buckling
JD-2-25	0.2	3.34	1.32	Channel plate and column core region buckling
JD-2-30	0.2	3.78	1.69	Beam buckling
JD-2-35	0.2	4.32	1.69	Beam buckling

4. Conclusions

Basing on the experiment of a new assembled joint between column and beam, finite element models are established to simulate this joint and analyse the effects of correlation parameters on its seismic performance. Following conclusions may be drawn:

(1) The joint studied has good ductility, energy dissipation capacity and bearing capacity when the ratio of axial compression stress to strength is not beyond 0.4.

(2) Increasing the thickness of channel will significantly raise the yield and ultimate load, initial stiffness, ductility and energy dissipation coefficient of joint.

References

[1] Hao J P, Sun X L, Xue Q, Fan C L 2017 Research and application of assembled steel structure building systems, *Eng. Mech.* **34** 1-13.
[2] Yan W, Cao Y H, Li G. R 2004 Development of assembly-type RC structure and building industrialization *J-Chongqingv Jianzhu Uni* **26** 131-36.
[3] Liu X. C, Pu S. H, Xu A. X, Ni Z, Zhang A L, Yang Z W 2015 Experimental study on static and seismic performance of bolted joint in modularized multi-layer and high-rise assembled steel structures, *J. Build. Struct.* **36(12)** 43-51.
[4] Wang X, Li H, Jiang C 2003 Hysteretic behavior of angles beam-column connections, *J. Huazhong Uni. Sci. Technol. (Natur. Sci. Edi.)* **31(8)** 13-5.
[5] Xin B U, Qian G U, Wang X W 2017 Cyclic Behavior of Spatial Beam-to-side Column Joint with T-stub, *DEStech Transc. Mater. Sci. Eng. (ICMSEA_MCE).*
[6] Li L M, Chen Y Y, Li N, Cai Y C 2010 Seismic performance of outer-shell connection of cold-formed square tubular column and H-shaped steel beam, *J. Jilin Uni (Eng. Technol. Edi.)* **40(1).**
[7] Li G Q, Duan L, Lu Y, Zhang L 2015 Experimental and theoretical study of bearing capacity for extended endplate connections between rectangular tubular columns and H-shaped beams with single direction bolts, *J. Build. Struct.* **36** 91-100.
[8] Yang C, Yang J F, Su M Z, Liu C Z 2016 Numerical study on seismic behaviours of ConXL biaxial moment connection, *J. Constr. Steel Res.* **121** 185-201.
[9] Rezaeian A, Omidi M J, Shahidi F 2014 Seismic behavior of ConXL rigid connection in box-columns not filled with concrete, *J. Constr. Steel Res.* **97** 79-104.
[10] Yang J F, Chen L, Cheng J P, Zhan Y H, Yan X F 2017 Experimental study on seismic behavior of a new type of fully assembled beam-column joints, *Eng. Mech.* **34** 75-86.